Article

A Comprehensive Weightbearing Computed Tomography Study on Patients With Hallux Valgus: Exploring Multiplanar Deformity Interrelationships

Chien-Shun Wang, MD[1,2] (iD), Erik Jesús Huánuco Casas, MD[3,4],
Emily J. Luo, BS[3] (iD), Antoine S. Acker, MD[3,5] (iD), Mark E. Easley, MD[3],
and Cesar de Cesar Netto, MD, PhD[3] (iD)

Abstract

Background Hallux valgus (HV) is a complex, multiplanar deformity. In this study, we examined the interrelationships between various components of this deformity using weightbearing computed tomography (WBCT). We hypothesized that the severity of traditional axial plane deformities would correlate with malpositioning of the metatarsosesamoid complex, first-ray coronal rotational deformity, and malalignment of the hindfoot and midfoot. The findings may offer valuable insights for guiding the correction of HV deformities.

Methods Patients with an HV angle greater than 15 degrees who underwent WBCT were included. Traditional 2-dimensional parameters were semiautomatically assessed. Manual measurements included hindfoot and midfoot WBCT parameters, for example, foot and ankle offset, talar posterior and middle facet morphology, and forefoot arch angle. First-ray parameters, including first metatarsal rotation, sesamoid rotation angle, hallucal pronation angle, and sesamoid position, were measured using established methods. Patients were categorized by hindfoot moment arm values to evaluate hindfoot-forefoot relationships.

Results Sixty-eight feet (53 patients) were included. Manual measurements exhibited excellent interobserver reliability, with ICCs of 0.845 to 0.987 and a kappa coefficient of 0.899 for the sesamoid position. The mean HV angle was 27.4 ± 7.8 degrees, whereas the mean IM angle was 15.8 ± 3.5 degrees. Significant correlations were observed between the HV and intermetatarsal (IM) angles, with all metatarsosesamoid complex parameters and first-ray coronal plane rotational parameters distal to the metatarsal head. The axial and sagittal talar–first metatarsal angles correlated with the HV angle but not with the IM angle. Significant differences in the HV angle, sagittal first tarsal–metatarsal joint angle, and first metatarsal head rotation were observed between the hindfoot moment arm groups, as confirmed by post hoc analysis.

Conclusion The findings support our hypothesis, identifying significant correlations between metatarsosesamoid complex malposition, distal first-ray coronal pronation, and traditional axial plane deformities in HV. Some hindfoot–midfoot alignments correlated with the HV angle but not with the IM angle.

Level of Evidence: Level IV: case series.

Keywords: first-ray pronation, hallux valgus, progressive collapsing foot deformity, sesamoid, weightbearing computed tomography

[1]Division of Orthopaedic Trauma, Department of Orthopaedics and Traumatology, Taipei Veterans General Hospital, Taipei, Taiwan

[2]Department of Orthopaedics, School of Medicine, National Yang Ming Chiao Tung University, Taipei, Taiwan

[3]Division of Foot and Ankle, Department of Orthopaedic Surgery, Duke University School of Medicine, Durham, NC, USA

[4]Department of Traumatology and Orthopedics, Delgado Clinic, Lima, Perú

[5]Centre of Foot and Ankle Surgery, Clinique La Colline, Geneva, Switzerland

Corresponding Author:
Cesar de Cesar Netto, MD, PhD, Division of Foot and Ankle, Department of Orthopaedic Surgery, Duke University School of Medicine, 2927 40 Duke Medicine Circle, 124 Davison Building, Durham, NC 27710, USA.
Email: cesar.netto@duke.edu

Introduction

Hallux valgus (HV) is a complex, multiplanar deformity characterized by axial plane deformities,[5] such as increased HV and intermetatarsal (IM) angles, as well as metatarso-sesamoid complex malposition[5,25,26] and first-ray coronal plane rotational deformities.[6,16,48,49,51] Although axial deformities are often clinically apparent, the latter 2 components require imaging for accurate diagnosis and assessment of structural implications.

The sesamoid position relative to the metatarsal head in traditional 2-dimensional anteroposterior radiographic views, as classified by Hardy and Clapham,[12] is crucial for predicting deformity recurrence after HV correction.[33,43] However, Kim et al[16] reported potential inaccuracies due to pseudo-subluxation when using planar radiography for evaluation. Additionally, previous studies on HV rotational deformities have predominantly focused on first metatarsal head rotational deformity, which increases recurrence risk and worsens outcomes.[3,32,34,35] If metatarsal head pronation and HV axial deformities share similar underlying pathologies and durations, a positive correlation between their severities would be expected. However, their correlation with the HV angle, IM angle, or sesamoid position have shown only weak or no significance.[16,21,24,29]

Among factors influencing the metatarsosesamoid complex, the lateralizing soft tissue vector pull is an important determinant of its position. The hindfoot, as the origin of the flexor hallucis brevis, abductor hallucis, and adductor hallucis, also influences the pathway of the flexor hallucis longus, potentially affecting sesamoid positioning. Moreover, Lalevée et al[20] found that rotational deformities in patients with HV can extend proximally to the navicular bone, highlighting differences in medial column rotation between patients with HV with and without progressive collapsing foot deformity. Coupled with previous findings on the correlation between hindfoot moment arm and first metatarsal head rotation,[1,45] these insights warrant further investigation into the relationship between hindfoot and midfoot alignment and HV axial plane deformities.

In this study, we employed weightbearing computed tomography (WBCT) to investigate first-ray structural deformities and midfoot and hindfoot alignments in patients with HV deformities. We aimed to assess the interrelationship between the severity of apparent axial plane deformities and other subtle abnormalities to guide correction planning. We hypothesized that HV axial plane deformity severity would positively correlate with metatarsosesamoid complex, first-ray rotational deformities, and hindfoot and midfoot malalignment.

Materials and Methods

This retrospective analysis was approved by the Institutional Review Board of the enrolling institution, with informed consent waived because of the retrospective nature of this study. Patients aged ≥18 years with HV angle >15 degrees who underwent WBCT at our institution between May 2023 and April 2024 were included. WBCT was indicated for suspected rotational deformity, including isolated HV deformity. Exclusion criteria included a history of ipsilateral foot or ankle surgeries and grade 4 midfoot arthritis per the Kellgren-Lawrence Grading Scale.[14] Demographic data such as age, sex, and body mass index (BMI) were collected through chart review.

Radiographic Evaluation

Cone-beam CT extremity scanners (pedCAT or HiRise model; CurveBeam, Warrington, PA) were used to conduct WBCT scans. The collected data sets were reviewed and converted into Digital Imaging and Communications in Medicine files with integrated software (CubeVue; CurveBeam). Parameters, including the talar–first metatarsal angle (axial and sagittal), calcaneal inclination angle,[40] hindfoot moment arm,[39] hindfoot angle, axial talonavicular angle, sagittal first tarsal–metatarsal angle, first tarsal–metatarsal joint minimum gap, IM angle, and HV angle, were semiautomatically assessed using DISIOR Bonelogic Foot and Ankle software (version 2.1.4, Helsinki, Finland), as detailed previously.[18,54]

Manual measurements were independently, randomly, and masked performed by 2 fellowship-trained foot and ankle surgeons using the CurveVue software. Pronation and supination were quantified as positive and negative rotation values, respectively. The measurement protocol and sequence are as follows (Figure 1):

1. Hindfoot and midfoot WBCT parameters:
    a. Foot and ankle offset[23] was automatically calculated using the Talus Alignment and Load Analysis System after the weightbearing points of the first and fifth metatarsal heads, the calcaneus, and the central and highest points of the talus were annotated.
    b. The CT slice with the largest cross-sectional area of the talus was selected for axis measurement. The axial and sagittal planes were aligned parallel to the talar long axis, defined by a line from the midpoint of the talar body to its head, first in the axial view and then, in the sagittal view. To assess talar facet parameters, the coronal plane was synchronized with the sagittal view at the midpoint of the facet's anterior-to-posterior dimension. Posterior facet measurements included the subtalar horizontal angle[36] (angle between the inferior facet and horizontal), the infratalar supratalar angle[36] (angle between the inferior and superior facets), and the infratalar supracalcaneal angle[36] (angle
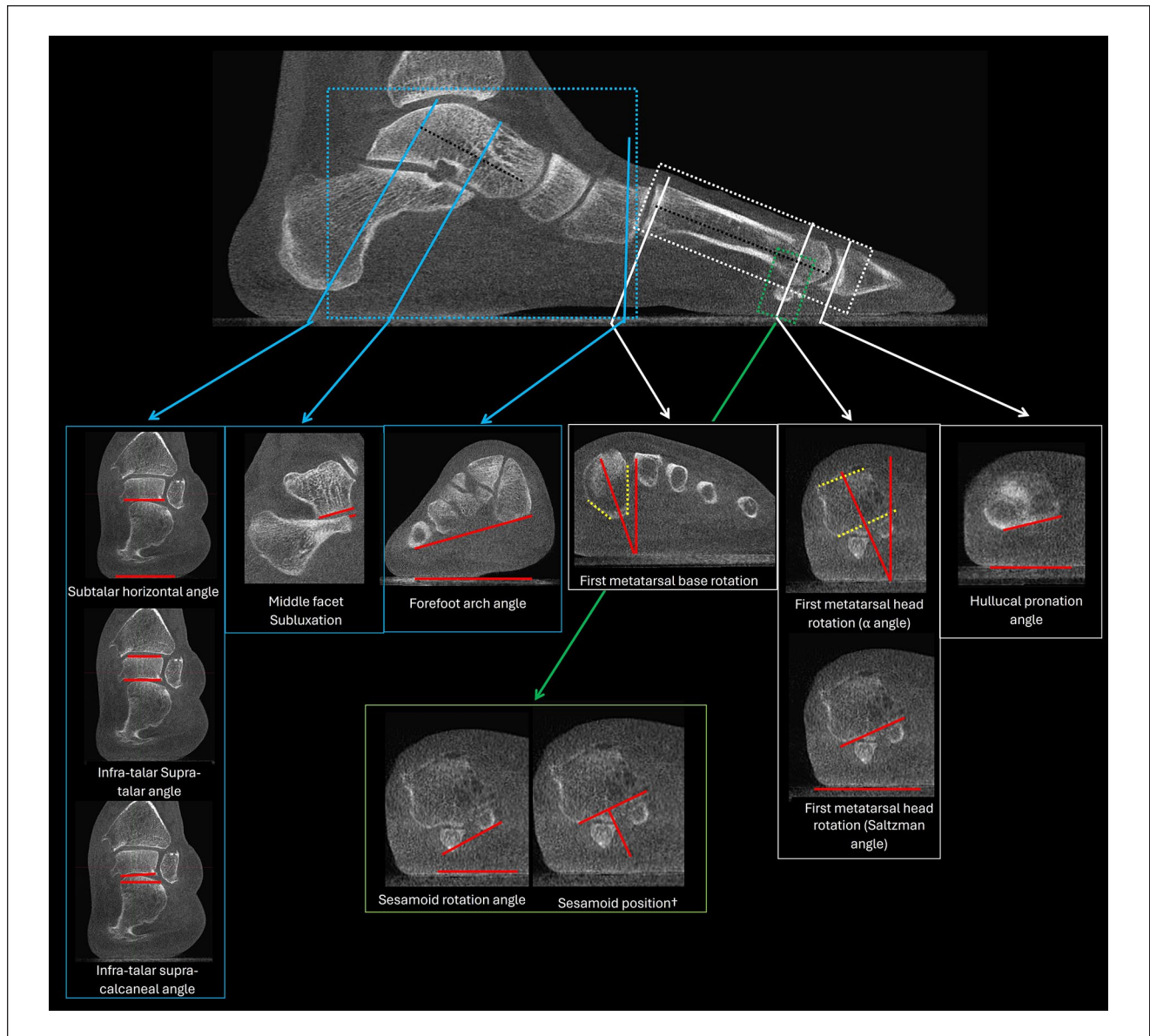
Figure 1. Illustrations of manual measurements. The black dashed lines indicate the bone axis, and the solid lines indicate the measurement levels. The blue lines denote hindfoot-midfoot weightbearing computed tomography parameters; the white lines indicate first-ray coronal plane rotational parameters; the green lines indicate metatarsosesamoid complex parameters; the yellow dashed lines represent tangential lines of the bone surface; and the red solid lines show each parameter measurement. † Four-stage grading system.[44,48,53]

between the inferior facet of the talus and the superior facet of the calcaneus). The middle facet uncoverage percentage[7] was calculated as the percentage of the talar articular surface not overlapped by the opposing calcaneal surface.

c. Realignment of the axial plane axis parallel to the second metatarsal's long axis and the sagittal plane axis parallel to ground level, following a previously described method for CT slice

determination, was performed to measure the forefoot arch angle[10] (angle between the horizontal and a line from the inferior aspect of the medial cuneiform to the inferior aspect of the fifth metatarsal).

2. First-ray parameters:

a. The axial and sagittal axes were aligned parallel to the first metatarsal's long axis on the CT image selected using prior technique. First

Table I. Intraclass Correlation Coefficient and Kappa Coefficient (95% CI) for Manual Measurements.

Manual measurements	Intraclass Correlation Coefficient and Kappa Coefficient (95% CI)
First metatarsal base rotation	0.966 (0.945-0.979)
First metatarsal head rotation (α angle)	0.956 (0.931-0.973)
First metatarsal head rotation (Saltzman angle)	0.921 (0.875-0.950)
Hallucal pronation angle	0.978 (0.964-0.986)
Sesamoid rotation angle	0.977 (0.963-0.986)
Sesamoid position[a]	0.899 (0.809-0.963)[b]
Foot and ankle offset	0.967 (0.948-0.980)
Subtalar horizontal angle	0.973 (0.956-0.983)
Infratalar supratalar angle	0.983 (0.973-0.990)
Infratalar supracalcaneal angle	0.883 (0.817-0.926)
Middle facet subluxation	0.945 (0.913-0.966)
Middle facet incongruence angle	0.845 (0.761-0.902)
Forefoot arch angle	0.987 (0.980-0.992)

[a]Four-stage grading system.[44,48,53]
[b]Kappa coefficient was used to calculate the agreement for the sesamoid position using the linear weighting and bootstrap method, with 95% CIs.

metatarsal base rotation[8,41] (angle between the vertical and a bisecting line of the angle formed by tangent lines to the medial and lateral surfaces of the first metatarsal bone just distal to the first tarsometatarsal joint), first metatarsal head α angle[16] (angle between the vertical line and the line connecting the midpoints of the medial and lateral dorsal corners and the midpoint of lateral and medial edges of the sulcus of the first metatarsal head), first metatarsal head Saltzman angle[38] (angle between the floor and the line connecting the lowest points of the lateral and medial edges of the sulcus of the first metatarsal head), sesamoid rotational angle[19] (angle between the floor and the tangential line of the most inferior aspect of the medial-lateral sesamoids), and hallux proximal phalanx rotation[8,41] (angle between the floor and the tangent line of the plantar aspect of the hallux proximal phalanx just distal to the metatarsal-phalangeal joint) were measured.

b. A 4-stage grading system[44,48,53] determined the sesamoid positions: grade 0 indicated tibial sesamoid entirely medial to the intersesamoid ridge; grade 1 indicated less than half the width of the tibial sesamoid subluxated laterally; grade 2 indicated more than half the width of the tibial sesamoid subluxated laterally; and

grade 3 indicated tibial sesamoid entirely lateral to the intersesamoid ridge.

c. The first metatarsal intrinsic rotation angle (determined by separately subtracting the first metatarsal base angle from the metatarsal head α angle and the Saltzman angle), first metatarsal-phalangeal joint rotation (determined by separately subtracting the metatarsal head α angle and the Saltzman angle from the hallux proximal phalanx rotation angle), and the metatarsal sesamoid rotation angle (determined by subtracting the metatarsal head Saltzman angle from the sesamoid rotational angle) were also calculated.

To further evaluate the relationship between the hindfoot and forefoot, patients were categorized according to their hindfoot moment arm values using criteria established from the mean and SD of assessments in a large-scale study of normative participants.[2] The classifications were as follows: group A represented varus (hindfoot moment arm less than 0.9 mm); group B denoted normal varus (0.9-6.12 mm); group C indicated normal valgus (6.12-11.34 mm); group D described valgus (11.34-16.35 mm); and group E indicated severe valgus (≥16.35 mm), equivalent to 1.96 times the SD from previous reports.

Statistical Analyses

Statistical analyses were conducted using SPSS software (Statistical Product and Service Solutions, version 25.0; IBM Corp, Armonk, NY). Interobserver reliability was quantified using the intraclass correlation coefficient (ICC), whereas agreement for sesamoid position was assessed using the kappa coefficient with linear weighting and the bootstrap method. The normality of variables was evaluated using the Shapiro-Wilk test and visual inspection of distribution histograms. Continuous variables were reported as means ± SD for normally distributed data and as medians with interquartile ranges (IQRs) for nonnormally distributed data. Categorical variables were expressed as numbers and percentages. Associations between normally distributed variables were analyzed using Pearson correlation coefficients, and Spearman correlation coefficients were used for nonnormally distributed and ordinal variables. Because of the exploratory nature of the study, the Holm-Bonferroni method[13] was used to control the false discovery rate and establish significance thresholds, considering only correlation coefficients with *P* values below these thresholds as statistically significant. Variability among hindfoot alignment groups was compared using the Kruskal-Wallis *H* test, with post hoc analyses to adjust for multiple comparisons across groups conducted using Dunn test with
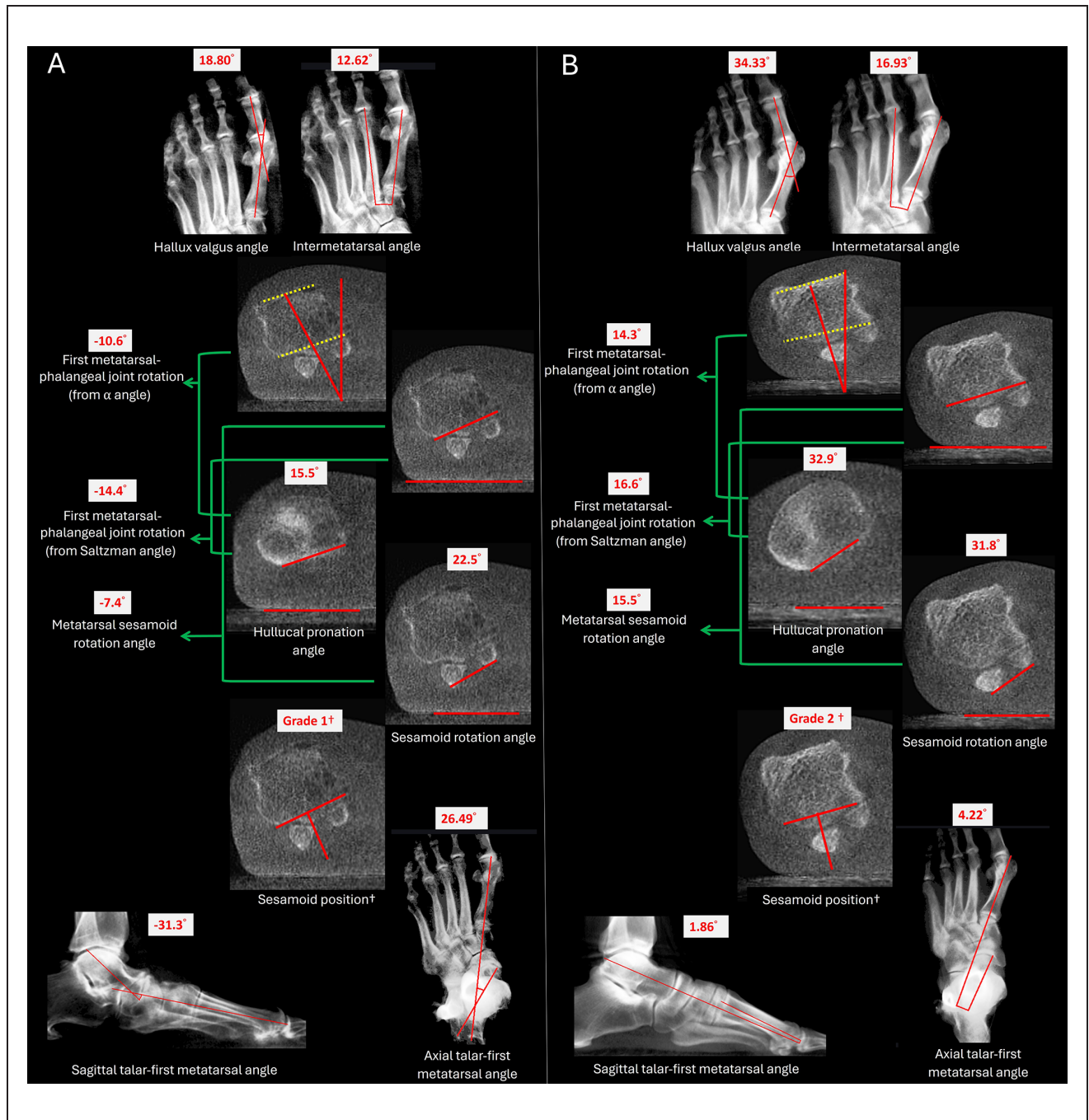
Figure 2. Illustrations of parameters significantly correlated with the hallux valgus angle and the intermetatarsal angle. The yellow dashed lines represent tangent lines of the bone surface. The solid red lines indicate the measurements of each parameter. The parameters indicated by the green arrows represent the difference between the 2 indicated parameters. The numbers shown in red denote the parameter values. Pronation is recorded as a positive value. (A) A 71-year-old female patient and (B) a 38-year-old male patient. † Four-stage grading system.[44,48,53]

Bonferroni correction. Statistical significance for tests between groups was set at $P < .05$ (2-tailed).

Results

Sixty-eight cases (53 patients) were analyzed, of which 41 (77.36%) involved female patients and 32 (47.1%) were left-sided. The median patient age was 60.5 years (IQR: 19.0), and the median BMI was 30.85 (IQR: 9.52). Manual measurements exhibited excellent interobserver reliability, with ICCs of 0.845-0.987 and a kappa coefficient of 0.899 for the sesamoid position (Table 1). The mean HV angle was 27.38 ± 7.83 degrees, whereas the mean IM angle was 15.80 ± 3.53 degrees.

All metatarsosesamoid complex malposition parameters, including sesamoid position, metatarsal sesamoid rotation angle, and sesamoid rotation angle, were significantly correlated with the HV and IM angles. First-ray coronal plane rotation parameters distal to the metatarsal head, including first metatarsal-phalangeal joint rotation (Saltzman and α angles) and hallucal pronation angle, showed significant correlations with the HV and IM angles. The axial and sagittal talar–first metatarsal angles demonstrated significant correlations with the HV angle but not with the IM angle (Figures 2 and 3, Table 2).

Details of the groupings are listed in Table 3. Group comparisons revealed no significant differences in age, BMI, and IM angle. However, the HV angle showed significant differences ($P = .003$), with post hoc analysis identifying significant differences between groups C and D ($P = .006$) and groups B and D ($P = .033$). Furthermore, the sagittal first tarsal–metatarsal joint angle showed significant differences ($P = .001$), with post hoc comparisons indicating significant differences between groups A and D ($P = .007$), A and E ($P = .041$), and B and D ($P = .015$). The first metatarsal head rotation (α angle) exhibited significant differences ($P = .004$), primarily between groups B and D ($P = .049$) and groups B and E ($P = .007$). The first metatarsal head rotation (Saltzman angle) also showed significant differences ($P = .004$), with differences between groups B and D ($P = .009$) and groups B and E ($P = .049$). Other parameters, including first metatarsal base rotation and first metatarsal bone rotation (Saltzman angle), showed significant differences in the Kruskal-Wallis *H* test but not in post hoc analysis (Table 4).

Discussion

Our results supported our hypothesis, indicating that the first metatarsal-phalangeal joint rotation (Saltzman angle) had the highest correlation with the HV angle ($r = 0.776$), whereas the hallucal pronation angle had the highest correlation with the IM angle ($r = 0.572$). Meanwhile, the first

metatarsal–phalangeal joint rotation, sesamoid position, metatarsal sesamoid rotation angle, hallucal pronation angle, and sesamoid rotation angle demonstrated significant correlations with both HV and IM angles. However, only the axial and sagittal talar–first metatarsal angles were significantly correlated with the HV angle, whereas no significant correlations were found between the midfoot and hindfoot parameters and IM angle. Significant differences in HV angle were observed between the groups classified by hindfoot moment arm severity, although the relationship did not show a consistent incremental change. The lowest median HV angle was found in the valgus group rather than in the varus or severe valgus groups. Furthermore, significant differences were observed only in parameters related to the coronal rotation of the first metatarsal head and sagittal first tarsal-metatarsal joint angle.

Since the 1990s, metatarsal pronation has been recognized as crucial to HV deformity.[9,47] Many corrective procedures aimed at supinating the first metatarsal have been applied in HV treatment.[4,42,50,52] However, their clinical significance remains controversial. First, most studies linking metatarsal head pronation to higher recurrence rates after HV surgery were based on indirect observations of the first metatarsal head shape,[32,34] the accuracy of which in reflecting true rotation is debated.[27] Second, a wide range of first metatarsal pronation is observed in patients without HV,[24,31,46] complicating the definition of normal values[21] and assessing clinical importance. Third, metatarsal pronation was previously thought to destabilize the metatarsosesamoid complex,[15,16] potentially inducing arthritis. However, recent studies using a 4-stage grading system[44,48,53] found no correlation between first metatarsal pronation and sesamoid subluxation.[21,29] Fourth, recent studies have observed compensatory supination of the first metatarsal during weightbearing in patients with HV.[11,17,22] In summary, the impact of this compensatory supination on first-ray stability may not be as significant as previously thought.

In our study, we observed no correlation between first metatarsal rotation and the severity of axial-plane HV deformities, in consistency with findings from previous studies.[13,18,21] However, more distal rotational parameters, such as first metatarsal-phalangeal joint rotation, hallucal pronation, and parameters related to the metatarsosesamoid complex (including the sesamoid rotation angle, metatarsal sesamoid rotation angle, and sesamoid position), were significantly correlated with both HV and IM angles. The first metatarsal-phalangeal joint rotation may result from medial joint capsule attenuation, whereas hallucal pronation may alter the insertion of the flexor hallucis longus, increasing the mediolateral vector of the forces.[37,48] Sesamoid rotation and lateral shifting suggest imbalances between the deep transverse metatarsal ligament, IM ligament,[30] and medial
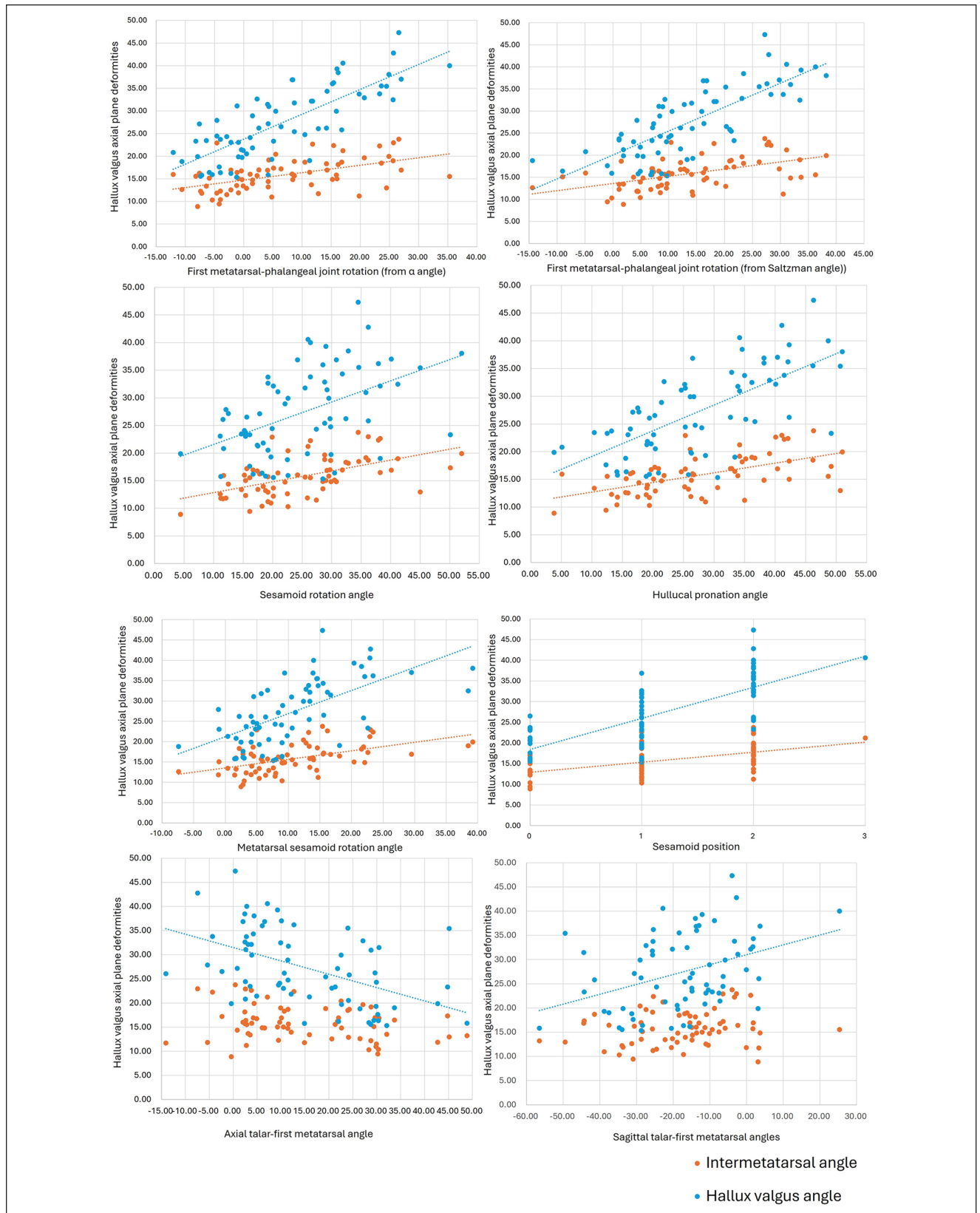
Figure 3. Illustrations of parameters significantly correlated with the hallux valgus angle and the intermetatarsal angle. Scatter plots display correlations between various parameters and the hallux valgus angle (blue dots) and the intermetatarsal angle (orange dots). The dotted lines represent the trend lines for each parameter.

Table 2. Correlation Coefficients for Parameters With the HV and IM Angles.

	Mean ± SD or Median (IQR)	HV Angle			IM Angle		
		Correlation Coefficient	P Value	Holm P Value Threshold[13]	Correlation Coefficient	P Value	Holm P Value Threshold[13]
Semiautomated measured parameters							
Axial talar–first metatarsal angle, degrees	11.42 (23.76)	ρ = −0.519	<.001*	.003	ρ = −0.221	.071	.003
Sagittal talar–first metatarsal angle, degrees	−17.71 ± 14.57	r = 0.379	.001*	.003	r = 0.186	.129	.003
Calcaneal inclination angle, degrees	16.31 ± 6.61	r = 0.253	.037	.005	r = 0.186	.129	.003
Hindfoot moment arm, mm	8.59 ± 8.07	r = −0.324	.007	.004	r = −0.178	.145	.004
Hindfoot angle, degrees	25.39 (10.43)	ρ = −0.331	.006	.004	ρ = −0.237	.052	.003
Axial talonavicular angle, degrees	41.53 ± 11.94	r = −0.256	.035	.004	r = −0.147	.233	.005
Sagittal first tarsal-metatarsal joint angle, degrees	8.93 ± 3.14	r = −0.090	.460	.013	r = 0.115	.349	.006
First tarsal-metatarsal joint minimum gap, mm	1.02 (0.28)	ρ = −0.076	.540	.017	ρ = 0.041	.741	.05
Hindfoot-midfoot weightbearing computed tomography parameters							
Foot and ankle offset, %	5.23 ± 4.3	r = −0.330	.006	.003	r = −0.080	.517	.013
Subtalar horizontal angle, degrees	6.45 ± 10.56	r = −0.348	.004	.003	r = −0.148	.230	.005
Infratalar supratalar angle, degrees	7.56 ± 14.95	r = −0.336	.005	.003	ρ = −0.161	.189	.004
Infratalar supracalcaneal angle, degrees	−2.45 ± 4.74	r = 0.118	.339	.006	r = 0.098	.427	.01
Middle facet subluxation, %	23.85 (14.24)	ρ = −0.110	.371	.008	ρ = −0.111	.366	.008
Forefoot arch angle, degrees	−6.43 ± 7.11	r = −0.232	.057	.005	r = −0.055	.656	.017
First-ray parameters							
First metatarsal base rotation, degrees	24.5 (8.88)	ρ = −0.106	.390	.01	ρ = −0.043	.730	.025
First metatarsal head rotation (α angle), degrees	21.23 ± 6.24	r = −0.145	.238	.006	r = 0.122	.321	.006
First metatarsal head rotation (Saltzman angle), degrees	14.26 ± 7.17	r = −0.112	.361	.007	r = 0.115	.350	.007
First metatarsal bone rotation (α angle), degrees	−3.16 ± 6.89	r = −0.038	.758	.025	r = 0.160	.192	.004
First metatarsal bone rotation (Saltzman angle), degrees	−11.65 (7.05)	ρ = 0.001	.992	.05	ρ = 0.217	.076	.003
First metatarsal-phalangeal joint rotation (α angle), degrees	4.25 (17.55)	ρ = 0.775	<.001*	.002	ρ = 0.539	<.001*	.002
First metatarsal-phalangeal joint rotation (Saltzman angle), degrees	13.53 ± 11.2	r = 0.776	<.001*	.002	r = 0.516	<.001*	.002
Sesamoid rotation angle, degrees	25.11 ± 9.82	r = 0.481	<.001*	.002	r = 0.548	<.001*	.002
Hallucal pronation angle, degrees	27.79 ± 11.55	r = 0.683	<.001*	.002	r = 0.572	<.001*	.002
Metatarsal sesamoid rotation angle, degrees	9.05 (10.8)	ρ = 0.685	<.001*	.002	ρ = 0.550	<.001*	.002
Sesamoid position[a]	1 (1)	ρ = 0.718	<.001*	.003	ρ = 0.502	<.001*	.003

Abbreviations: HV, hallux valgus; IM, intermetatarsal; ρ (rho), Spearman rank correlation coefficient; r, Pearson correlation coefficient.
[a]According to the 4-stage grading system.44,48,53
*P value < Holm P value threshold.

Table 3. Details of Grouping by Hindfoot Moment Arm Severity.

Group	Hindfoot Moment Arm (mm)	Number	Median (IQR)
A: Varus	<0.9	10	−2.16 (3.44)
B: Normal varus	0.9-6.12	19	3.29 (2.79)
C: Normal valgus	6.12-11.34	16	9.03 (2.59)
D: Valgus	11.34-16.35	13	13.87 (2.8)
E: Severe valgus	≥16.35	10	23.25 (4.42)

Abbreviation: IQR, interquartile range.

joint capsule, causing malfunction in the flexor hallucis brevis, hallux adductor, and abductor due to altered trajectories. These findings support the notion that the severity of HV axial plane deformity is significantly associated with soft tissue dysfunction. The lack of an incremental relationship between the first metatarsal rotation and HV axial plane deformity may stem from 2 factors. First, the first metatarsal is neither the origin nor the insertion of the hallux muscles; therefore, its malrotation has a limited impact on muscle vector direction. Second, in patients with HV, the relatively attenuated metatarsal-phalangeal joint capsule may reduce its influence on the axial plane deformity.

Regarding midfoot and hindfoot anatomic characteristics, we found a significant correlation between the axial and sagittal talar-first metatarsal and HV angles. Despite the typically larger IM angle in patients with HV, the axial talar–first metatarsal angle showed no correlation with the IM angle, likely because of the inward alignment of the first metatarsal relative to the hindfoot, which increases the lateral forces on the hallux, thereby facilitating an increase in the HV angle. Najefi et al[29] observed a weak positive correlation between the IM angle and hindfoot valgus in patients with HV. Conversely, we observed a weak negative correlation of a planovalgus foot shape (higher axial and lower sagittal talar-first metatarsal angles) with the HV angle but no correlation with the IM angle. This discrepancy may be attributed to cohort differences—our patients generally had more valgus hindfoot alignment (mean hindfoot angle of 27.13 degrees compared with 10.4 degrees in the study above), with 57% (39/68) exhibiting a hindfoot moment arm exceeding 6.12 mm. Meanwhile, more severe deformity did not correspond to a lower HV angle when comparing hindfoot moment arm severity groups. Thus, the relationship between hindfoot alignment and HV angle is not straightforward. The causes of HV may differ depending on hindfoot alignment (valgus or varus). Although higher hindfoot moment arm groups had higher first metatarsal head pronation, consistent with previous research,[1] they did not exhibit a higher HV angle. Furthermore, no significant differences were identified among different hindfoot moment arm groups on parameters correlated to the HV and IM angles, such as first metatarsal-phalangeal

joint rotation, hallucal pronation, and metatarsosesamoid complex parameters. This could explain why patients with progressive collapsing foot deformities do not necessarily develop HV.

This study has several limitations. First, as a cross-sectional cohort study, it identified significant correlations between metatarsosesamoid complex malposition, first ray coronal plane rotational deformity, and traditional axial plane deformities. However, causal relationships could not be established. Second, the inclusion criteria focused on patients with an HV angle exceeding 15 degrees rather than those with HV symptoms, which might have introduced bias or reduced clinical relevance. However, the severity of HV deformity does not necessarily correlate with symptom manifestation.[28] As we aimed to observe the relationship between various deformities, this inclusion criterion minimally impacted our conclusions. Third, the small sample size in each subgroup may have introduced potential errors. Finally, we primarily measured WBCT parameters without directly including soft tissue conditions. Additional imaging studies, such as magnetic resonance imaging and dynamic studies, should be included in future research for a more comprehensive assessment.

In conclusion, the severity of axial plane deformities in patients with HV significantly correlated with more distal coronal rotational deformities, including metatarsophalangeal joint pronation, hallucal pronation, and metatarsosesamoid complex malposition, but not with the degree of first metatarsal head pronation. These findings offer clinicians a framework for estimating rotational deformity severity through 2-dimensional imaging, providing a reference for planning hallux valgus correction. Among midfoot and hindfoot alignments, the axial and sagittal talar-first metatarsal angles showed correlation with the HV angle but not with the IM angle. Additionally, similar HV axial plane deformity-correlated parameters were observed among the groups based on the hindfoot moment arm, partially explaining why not all patients with hindfoot valgus developed HV deformities. A potential value of this study is its use as an exploratory analysis for future research. Based on the number of significantly correlated parameters (7 continuous variables and 1 categorical variable) identified in this study

Table 4. Comparison of First-Ray Parameters Across Hindfoot Moment Arm Severity Groups.

Parameter	Group	Median (IQR)	Kruskal-Wallis *H* Test		Post Hoc Dunn Test Results	
			Test Statistic	P Value	Comparison	P Value[a]
Age, y	A	61.5 (14)	4.788	.310	N/A	
	B	55 (38)				
	C	57 (31)				
	D	65 (15)				
	E	64 (13)				
Body mass index	A	31.63 (8.85)	9.330	.053	N/A	
	B	26.52 (12.59)				
	C	29.63 (8.6)				
	D	32.49 (12.61)				
	E	34.08 (7.42)				
Hallux valgus angle, degrees	A	30.51 (11.79)	16.38	.003**	A vs B	>.999
					A vs C	>.999
	B	27.89 (10.87)			A vs D	.160
					A vs E	.999
	C	31.82 (12.62)			B vs C	>.999
					B vs D	.033*
	D	19.72 (8.29)			B vs E	.456
					C vs D	.006**
	E	23.08 (9.38)			C vs E	.133
					D vs E	>.999
Intermetatarsal angle, degrees	A	16.11 (5.17)	8.478	.076	N/A	
	B	14.86 (4.47)				
	C	17.56 (3.76)				
	D	15.04 (5.26)				
	E	13.25 (5.51)				
Sagittal first tarsal–metatarsal joint angle, degrees	A	6.84 (3.17)	18.424	.001**	A vs B	>.999
					A vs C	.786
	B	6.96 (6.77)			A vs D	.007**
					A vs E	.041*
	C	9.33 (3.9)			B vs C	>.999
					B vs D	.015*
	D	10.65 (2.68)			B vs E	.112
					C vs D	.528
	E	10.09 (3.09)			C vs E	>.999
					D vs E	>.999
First tarsal–metatarsal joint minimum gap, mm	A	1.05 (0.44)	1.161	.885	N/A	
	B	1.01 (0.27)				
	C	1.03 (0.34)				
	D	1.03 (0.21)				
	E	0.97 (0.28)				
First metatarsal base rotation, degrees	A	22.15 (7.73)	10.152	.038*	A vs B	>.999
					A vs C	.706
	B	22 (6.2)			A vs D	.959
					A vs E	.087
	C	25.65 (9.93)			B vs C	>.999
					B vs D	>.999
	D	24.7 (5.45)			B vs E	.118
					C vs D	>.999
	E	28.65 (13.68)			C vs E	>.999
					D vs E	>.999

(continued)

Table 4. (continued)

| Parameter | Group | Median (IQR) | Kruskal-Wallis *H* Test | | Post Hoc Dunn Test Results | |
			Test Statistic	*P* Value	Comparison	*P* Value[a]
First metatarsal head rotation (α angle), degrees	A	18.65 (13.18)	15.492	.004**	A vs B	>.999
					A vs C	>.999
	B	17.2 (8.2)			A vs D	.718
					A vs E	.162
	C	19.8 (8.13)			B vs C	.914
					B vs D	.049*
	D	21.6 (6.2)			B vs E	.007*
					C vs D	>.999
	E	25.5 (5.73)			C vs E	.601
					D vs E	>.999
First metatarsal head rotation (Saltzman angle), degrees	A	11.9 (8.35)	15.635	.004**	A vs B	>.999
					A vs C	>.999
	B	9.3 (8.7)			A vs D	.263
					A vs E	.620
	C	12.9 (10.08)			B vs C	.213
					B vs D	.009**
	D	16.4 (11.35)			B vs E	.049*
					C vs D	>.999
	E	17.5 (7.93)			C vs E	>.999
					D vs E	>.999
First metatarsal bone rotation (α angle), degrees	A	−4 (13.25)	1.796	.773	N/A	
	B	−5.1 (6.7)				
	C	−3.45 (9.18)				
	D	−3 (8.2)				
	E	−0.2 (13.8)				
First metatarsal bone rotation (Saltzman angle), degrees	A	−10.85 (7.18)	9.534	.049*	A vs B	>.999
					A vs C	>.999
	B	−13.2 (6.7)			A vs D	>.999
					A vs E	>.999
	C	−10.95 (8.58)			B vs C	.915
					B vs D	.074
	D	−7 (9.95)			B vs E	>.999
					C vs D	>.999
	E	−13.4 (6.88)			C vs E	>.999
					D vs E	.169
First metatarsal–phalangeal joint rotation (α angle), degrees	A	7.9 (28.03)	7.164	.127	N/A	
	B	8.4 (18.3)				
	C	11.15 (21.1)				
	D	−0.3 (9.75)				
	E	0.3 (9.83)				
First metatarsal–phalangeal joint rotation (Saltzman angle), degrees	A	10.5 (24.25)	6.834	.145	N/A	
	B	14.2 (16)				
	C	14.5 (16.8)				
	D	7 (13.55)				
	E	9.1 (12.2)				
Sesamoid rotation angle, degrees	A	23.65 (14.13)	6.765	.149	N/A	
	B	19.2 (16)				
	C	29.45 (11.45)				
	D	22.5 (19.6)				
	E	24.25 (9.2)				

Table 4. (continued)

| Parameter | Group | Median (IQR) | Kruskal-Wallis *H* Test | | Post Hoc Dunn Test Results | |
			Test Statistic	*P* Value	Comparison	*P* Value[a]
Hallucal pronation angle, degrees	A	26 (22.9)	5.237	.264	N/A	
	B	21.8 (16.7)				
	C	33.65 (22.85)				
	D	20.9 (19.15)				
	E	27.1 (12.8)				
Metatarsal sesamoid rotation angle, degrees	A	11.9 (17.8)	4.746	.314	N/A	
	B	9.8 (10.2)				
	C	13.35 (10.4)				
	D	5.9 (14.6)				
	E	7.75 (8.45)				
Sesamoid position[b]	A	1 (1)	5.125	.275	N/A	
	B	1 (2)				
	C	2 (1)				
	D	1 (2)				
	E	1 (0)				

Abbreviations: IQR, interquartile range; N/A, not applicable.
[a]Using Bonferroni adjustment.
[b]According to the 4-stage grading system.[44,48,53]
[*]$P < .05$.
[**]$P < .01$.

and the effect sizes calculated from the smallest squared correlation coefficients among these parameters, a minimum of 107 cases would be required under standard conditions if a structural equation model and mediation analysis are developed in the future to investigate the temporal and causal relationships among the various components of HV deformity.

Ethical Approval

Ethical approval for this study was obtained from the Duke University Health System Institutional Review Board (IRB number: Pro00113556).

Declaration of Conflicting Interests

The author(s) declared the following potential conflicts of interest with respect to the research, authorship, and/or publication of this article: Cesar de Cesar Netto, MD, PhD, holds financial interests related to CurveBeam, Paragon 28, and Disior, including but not limited to equity, royalties, advisory roles, and consultancy fees. These interests have been managed in accordance with relevant regulations and Duke University's policies. The author has entered into a conflict management plan with the relevant departments to ensure the objectivity of the research and the fairness of educational activities, as well as to uphold the reputation of Duke University. All other authors declare no conflicts of interest. Disclosure forms for all authors are available online.

ORCID iDs

Chien-Shun Wang, MD, (iD) https://orcid.org/0000-0001-8707-1108
Emily J. Luo, BS, (iD) https://orcid.org/0000-0003-2237-3521
Antoine S. Acker, MD, (iD) https://orcid.org/0000-0002-4103-6136
Cesar de Cesar Netto, MD, PhD, (iD) https://orcid.org/0000-0001-6037-0685

References

1. Bakshi N, Steadman J, Philippi M, et al. Association between hindfoot alignment and first metatarsal rotation. *Foot Ankle Int*. 2022;43(1):105-112. doi:10.1177/10711007211033514
2. Choi JY, Lee HI, Kim JH, Suh JS. Radiographic measurements on hindfoot alignment view in 1128 asymptomatic subjects. *Foot Ankle Surg*. 2021;27(4):366-370. doi:10.1016/j.fas.2020.04.010
3. Conti MS, Patel TJ, Zhu J, Elliott AJ, Conti SF, Ellis SJ. Association of first metatarsal pronation correction with patient-reported outcomes and recurrence rates in hallux valgus. *Foot Ankle Int*. 2022;43(3):309-320. doi:10.1177/10711007211046938

4. Conti MS, Willett JF, Garfinkel JH, et al. Effect of the modified Lapidus procedure on pronation of the first ray in hallux valgus. *Foot Ankle Int*. 2020;41(2):125-132. doi:10.1177/1071100719883325

5. Coughlin MJ. Hallux valgus. *J Bone Joint Surg Am*. 1996;78(6):932-966.

6. Dayton P, Kauwe M, DiDomenico L, Feilmeier M, Reimer R. Quantitative analysis of the degree of frontal rotation required to anatomically align the first metatarsal phalangeal joint during modified tarsal-metatarsal arthrodesis without capsular balancing. *J Foot Ankle Surg*. 2016;55(2):220-225. doi:10.1053/j.jfas.2015.08.018

7. de Cesar Netto C, Godoy-Santos AL, Saito GH, et al. Subluxation of the middle facet of the subtalar joint as a marker of peritalar subluxation in adult acquired flatfoot deformity: a case-control study. *J Bone Joint Surg Am*. 2019;101(20):1838-1844. doi:10.2106/JBJS.19.00073

8. Dibbern K, Briggs H, Behrens A, et al. Reliability of coronal plane rotation measurements in the medial column of the foot: a cadaveric study. *J Foot Ankle*. 2021;15(3):252-258.

9. Eustace S, O'Byrne J, Stack J, Stephens MM. Radiographic features that enable assessment of first metatarsal rotation: the role of pronation in hallux valgus. *Skeletal Radiol*. 1993;22(3):153-156. doi:10.1007/BF00206143

10. Ferri M, Scharfenberger AV, Goplen G, Daniels TR, Pearce D. Weightbearing CT scan of severe flexible pes planus deformities. *Foot Ankle Int*. 2008;29(2):199-204. doi:10.3113/FAI.2008.0199

11. Geng X, Wang C, Ma X, et al. Mobility of the first metatarsal-cuneiform joint in patients with and without hallux valgus: in vivo three-dimensional analysis using computerized tomography scan. *J Orthop Surg Res*. 2015;10:140. doi:10.1186/s13018-015-0289-2

12. Hardy RH, Clapham JC. Observations on hallux valgus; based on a controlled series. *J Bone Joint Surg Br*. 1951;33-B(3):376-391. doi:10.1302/0301-620X.33B3.376

13. Holm S. A simple sequentially rejective multiple test procedure. *Scand J Stat*. 1979;6(2):65-70.

14. Kellgren JH, Lawrence JS. Radiological assessment of osteoarthrosis. *Ann Rheum Dis*. 1957;16(4):494-502. doi:10.1136/ard.16.4.494

15. Kim JS, Young KW. Sesamoid position in hallux valgus in relation to the coronal rotation of the first metatarsal. *Foot Ankle Clin*. 2018;23(2):219-230. doi:10.1016/j.fcl.2018.01.003

16. Kim Y, Kim JS, Young KW, Naraghi R, Cho HK, Lee SY. A new measure of tibial sesamoid position in hallux valgus in relation to the coronal rotation of the first metatarsal in CT scans. *Foot Ankle Int*. 2015;36(8):944-952. doi:10.1177/1071100715576994

17. Kimura T, Kubota M, Taguchi T, Suzuki N, Hattori A, Marumo K. Evaluation of first-ray mobility in patients with hallux valgus using weight-bearing CT and a 3-D analysis system: a comparison with normal feet. *J Bone Joint Surg Am*. 2017;99(3):247-255. doi:10.2106/JBJS.16.00542

18. Krahenbuhl N, Kvarda P, Susdorf R, et al. Assessment of progressive collapsing foot deformity using semiautomated 3D measurements derived from weightbearing CT scans. *Foot Ankle Int*. 2022;43(3):363-370. doi:10.1177/10711007211049754

19. Kuwano T, Nagamine R, Sakaki K, Urabe K, Iwamoto Y. New radiographic analysis of sesamoid rotation in hallux valgus: comparison with conventional evaluation methods. *Foot Ankle Int*. 2002;23(9):811-817. doi:10.1177/107110070202300907

20. Lalevee M, Barbachan Mansur NS, Dibbern K, et al. Coronal plane rotation of the medial column in hallux valgus: a retrospective case-control study. *Foot Ankle Int*. 2022;43(8):1041-1048. doi:10.1177/10711007221091810

21. Lalevee M, de Carvalho KAM, Barbachan Mansur NS, et al. Distribution, prevalence, and impact on the metatarsosesamoid complex of first metatarsal pronation in hallux valgus. *Foot Ankle Surg*. 2023;29(6):488-496. doi:10.1016/j.fas.2023.06.003

22. Lalevee M, Dibbern K, Barbachan Mansur NS, et al. Impact of first metatarsal hyperpronation on first ray alignment: a study in cadavers. *Clin Orthop Relat Res*. 2022;480(10):2029-2040. doi:10.1097/CORR.0000000000002265

23. Lintz F, Welck M, Bernasconi A, et al. 3D biometrics for hindfoot alignment using weightbearing CT. *Foot Ankle Int*. 2017;38(6):684-689. doi:10.1177/1071100717690806

24. Mahmoud K, Metikala S, Mehta SD, Fryhofer GW, Farber DC, Prat D. The role of weightbearing computed tomography scan in hallux valgus. *Foot Ankle Int*. 2021;42(3):287-293. doi:10.1177/1071100720962398

25. Mann RA, Coughlin MJ. Hallux valgus—etiology, anatomy, treatment and surgical considerations. *Clin Orthop Relat Res*. 1981;157:31-41.

26. Mann RA, Pfeffinger L. Hallux valgus repair. Duvries modified McBride procedure. *Clin Orthop Relat Res*. 1991;272:213-218.

27. Mansur NSB, Lalevee M, Schmidt E, et al. Correlation between indirect radiographic parameters of first metatarsal rotation in hallux valgus and values on weight-bearing computed tomography. *Int Orthop*. 2021;45(12):3111-3118. doi:10.1007/s00264-021-05136-9

28. Matthews M, Klein E, Acciani A, et al. Correlation of preoperative radiographic severity with disability and symptom severity in hallux valgus. *Foot Ankle Int*. 2019;40(8):923-928. doi:10.1177/1071100719845002

29. Najefi AA, Katmeh R, Zaveri AK, et al. Imaging findings and first metatarsal rotation in hallux valgus. *Foot Ankle Int*. 2022;43(5):665-675. doi:10.1177/10711007211064609

30. Najefi AA, Malhotra K, Patel S, Cullen N, Welck M. Assessing the rotation of the first metatarsal on computed tomography scans: a systematic literature review. *Foot Ankle Int*. 2022;43(1):66-76. doi:10.1177/10711007211020676

31. Najefi AA, Zaveri A, Alsafi MK, et al. The assessment of first metatarsal rotation in the normal adult population using weightbearing computed tomography. *Foot Ankle Int*. 2021;42(10):1223-1230. doi:10.1177/10711007211015187

32. Okuda R, Kinoshita M, Yasuda T, Jotoku T, Kitano N, Shima H. The shape of the lateral edge of the first metatarsal head as a risk factor for recurrence of hallux valgus. *J Bone Joint Surg Am*. 2007;89(10):2163-2172. doi:10.2106/JBJS.F.01455

33. Okuda R, Kinoshita M, Yasuda T, Jotoku T, Kitano N, Shima H. Postoperative incomplete reduction of the sesamoids as a risk factor for recurrence of hallux valgus. *J Bone Joint Surg Am*. 2009;91(7):1637-1645. doi:10.2106/JBJS.H.00796

34. Okuda R, Yasuda T, Jotoku T, Shima H. Supination stress of the great toe for assessing intraoperative correction of hallux valgus. *J Orthop Sci*. 2012;17(2):129-135. doi:10.1007/s00776-011-0182-8

35. Ono Y, Yamaguchi S, Sadamasu A, et al. The shape of the first metatarsal head and its association with the presence of sesamoid-metatarsal joint osteoarthritis and the pronation angle. *J Orthop Sci*. 2020;25(4):658-663. doi:10.1016/j.jos.2019.06.013

36. Probasco W, Haleem AM, Yu J, Sangeorzan BJ, Deland JT, Ellis SJ. Assessment of coronal plane subtalar joint alignment in peritalar subluxation via weight-bearing multiplanar imaging. *Foot Ankle Int*. 2015;36(3):302-309. doi:10.1177/1071100714557861

37. Saltzman CL, Aper RL, Brown TD. Anatomic determinants of first metatarsophalangeal flexion moments in hallux valgus. *Clin Orthop Relat Res*. 1997(339):261-269. doi:10.1097/00003086-199706000-00035

38. Saltzman CL, Brandser EA, Anderson CM, Berbaum KS, Brown TD. Coronal plane rotation of the first metatarsal. *Foot Ankle Int*. 1996;17(3):157-161. doi:10.1177/107110079601700307

39. Saltzman CL, el-Khoury GY. The hindfoot alignment view. *Foot Ankle Int*. 1995;16(9):572-576. doi:10.1177/107110079501600911

40. Saltzman CL, Nawoczenski DA, Talbot KD. Measurement of the medial longitudinal arch. *Arch Phys Med Rehabil*. 1995;76(1):45-49. doi:10.1016/s0003-9993(95)80041-7

41. Schmidt E, Silva T, Baumfeld D, et al. The rotational positioning of the bones in the medial column of the foot: a weight-bearing CT analysis. *Iowa Orthop J*. 2021;41(1):103-109.

42. Seki H, Oki S, Suda Y, et al. Three-dimensional analysis of the first metatarsal bone in minimally invasive distal linear metatarsal osteotomy for hallux valgus. *Foot Ankle Int*. 2020;41(1):84-93. doi:10.1177/1071100719875222

43. Shibuya N, Kyprios EM, Panchani PN, Martin LR, Thorud JC, Jupiter DC. Factors associated with early loss of hallux valgus correction. *J Foot Ankle Surg*. 2018;57(2):236-240. doi:10.1053/j.jfas.2017.08.018

44. Smith RW, Reynolds JC, Stewart MJ. Hallux valgus assessment: report of research committee of American Orthopaedic Foot and Ankle Society. *Foot Ankle*. 1984;5(2):92-103. doi:10.1177/107110078400500208

45. Steadman J, Bakshi N, Philippi M, et al. Association of normal vs abnormal Meary angle with hindfoot malalignment and first metatarsal rotation: a short report. *Foot Ankle Int*. 2022;43(5):706-709. doi:10.1177/10711007211068473

46. Steadman J, Barg A, Saltzman CL. First metatarsal rotation in hallux valgus deformity. *Foot Ankle Int*. 2021;42(4):510-522. doi:10.1177/1071100721997149

47. Stephens MM. Coronal plane rotation of the first metatarsal. *Foot Ankle Int*. 1996;17(11):720-721.

48. Talbot KD, Saltzman CL. Hallucal rotation: a method of measurement and relationship to bunion deformity. *Foot Ankle Int*. 1997;18(9):550-556. doi:10.1177/107110079701800904

49. Wagner P, Ortiz C, Keller A, Zanolli D, Wangner E. Hallux valgus treatment: a tridimensional problem. *Tobillo Pie*. 2016;8(2):128-132.

50. Wagner P, Wagner E. Proximal rotational metatarsal osteotomy for hallux valgus (promo) short-term prospective case series with a novel technique and topic review. *Foot Ankle Orthop*. 2018;3(3):2473011418790071. doi:10.1177/2473011418790071

51. Yamaguchi S, Sasho T, Endo J, et al. Shape of the lateral edge of the first metatarsal head changes depending on the rotation and inclination of the first metatarsal: a study using digitally reconstructed radiographs. *J Orthop Sci*. 2015;20(5):868-874. doi:10.1007/s00776-015-0749-x

52. Yasuda T, Okuda R, Jotoku T, Shima H, Hida T, Neo M. Proximal supination osteotomy of the first metatarsal for hallux valgus. *Foot Ankle Int*. 2015;36(6):696-704. doi:10.1177/1071100715572188

53. Yildirim Y, Cabukoglu C, Erol B, Esemenli T. Effect of metatarsophalangeal joint position on the reliability of the tangential sesamoid view in determining sesamoid position. *Foot Ankle Int*. 2005;26(3):247-250. doi:10.1177/107110070502600311

54. Zaidi R, Sangoi D, Cullen N, Patel S, Welck M, Malhotra K. Semi-automated 3-dimensional analysis of the normal foot and ankle using weight bearing CT - a report of normal values and bony relationships. *Foot Ankle Surg*. 2023;29(2):111-117. doi:10.1016/j.fas.2022.12.001